J. Adhesion Sci. Technol., Vol. , No. , pp. 1–13 (2007)

Also available online - www.brill.nl/jast

Matrix-assisted pulsed-laser evaporation of DOPA-modified poly(ethylene glycol) thin films

A. DORAISWAMY [1], C. DINU [2], R. CRISTESCU [3], P. B. MESSERSMITH [4], B. J. CHISHOLM [5], S. J. STAFSLIEN [5], D. B. CHRISEY [6] and R. J. NARAYAN [1,*]

[1] *Department of Biomedical Engineering, University of North Carolina, 152 MacNider Hall, Campus Box 7575, Chapel Hill, NC 27599-7575, USA*
[2] *Max Planck Institute of Molecular Cell Biology and Genetics, Pfotenhauerstrasse, Dresden 01307, Germany*
[3] *Lasers Department, National Institute for Lasers, Plasma and Radiation Physics, Atomistilor 409, P.O. Box MG-36, Bucharest Magurele RO-077125, Romania*
[4] *Department of Biomedical Engineering, Northwestern University, 633 Clark Street, Evanston, IL 60208, USA*
[5] *Center for Nanoscale Science and Engineering, North Dakota State University, 1805 NDSU Research Park Drive, Fargo, ND 58102, USA*
[6] *Department of Materials Science and Engineering, Rensselaer Polytechnic Institute, 110 8th Street, Troy, NY 12180-3590, USA*

Received in final form 11 January 2007

Abstract—3,4-Dihydroxyphenyl-L-alanine-modified poly(ethylene glycol) (mPEG-$DOPA_3$) is a biologically-inspired material that exhibits unique adhesion properties. In this study, mPEG-$DOPA_3$ thin films were prepared using a novel laser process known as matrix-assisted pulsed-laser evaporation (MAPLE). The films were examined using Fourier transform infrared spectroscopy, atomic force microscopy, profilometry, antifouling studies and cell adhesion studies. The Fourier transform infrared spectroscopy data demonstrated that the main functional groups in the MAPLE-deposited mPEG-$DOPA_3$ films remained intact. Profilometry and atomic force microscopy studies confirmed that MAPLE provides excellent control over film morphology, as well as film thickness. High resolution patterns of mPEG-$DOPA_3$ thin films were obtained by masking. MAPLE-deposited mPEG-$DOPA_3$ thin films demonstrated an absence of cytotoxicity and acceptable antifouling properties against the marine bacterium *Cytophaga lytica*. MAPLE-deposited mPEG-$DOPA_3$ thin films potentially have numerous biomedical and marine applications.

Keywords: Mussel adhesive protein analog; thin films; matrix-assisted pulsed-laser evaporation; antifouling.

*To whom correspondence should be addressed. Tel.: (1-919) 696-8488; Fax: (1-919) 513-3814; e-mail: roger_narayan@unc.edu

1. INTRODUCTION

The use of acrylics, cyanoacrylates, epoxies, phenolics, polyurethanes, silicones and other synthetic adhesives is fraught with many health and environmental concerns. Synthetic adhesives that contain volatile organic solvents are being discontinued because of concerns that these materials may contribute to smog, atmospheric ozone depletion, respiratory injury and systemic toxicity [1–4]. Formaldehyde, a component in many synthetic adhesives, has been associated with leukemia, nasopharyngeal cancer, sinonasal adenocarcinoma, and squamous-cell carcinoma. *In vitro* and *in vivo* studies have shown that formaldehyde is genotoxic; for example, workers exposed to formaldehyde exhibited larger numbers of DNA–protein cross-links. In addition, synthetic adhesives contain petroleum, natural gas and other non-renewable precursors. Novel materials are being developed that reduce or eliminate the liabilities associated with synthetic adhesives [5]. Marine mussel adhesive protein is a natural material that has recently been considered for use as an alternative to conventional synthetic adhesives [6–11]. Mussels attach to surfaces by means of a byssus, a bundle of 5–50-mm-long threads. Each thread consists of a collagenous core that is coated with mussel adhesive proteins [12]. The blue mussel (*Mytilus edulis*) produces five unique proteins, *Mytilus edulis* foot protein-1, *Mytilus edulis* foot protein-2, *Mytilus edulis* foot protein-3, *Mytilus edulis* foot protein-4 and *Mytilus edulis* foot protein-5. 3,4-Dihydroxyphenyl-L-alanine (L-DOPA) residues have been shown to be responsible for the adhesive properties of *Mytilus edulis* foot protein-1. This approx. 110-kDa material contains 20% lysine, 15% L-DOPA; and 30–50% hydroxyproline, threonine and tyrosine. These amino acids appear in hexapeptide and decapeptide motifs that repeat up to eighty times within the protein. Mussel adhesive proteins demonstrate high adhesion strength to many metals, metal oxides, polymers and glasses in aqueous environments [13–15]. The hydroxyl groups in L-DOPA may chelate with metal or stainless steel surfaces and may form hydrogen bonds with metal oxide surfaces. In addition, the L-DOPA groups may be oxidized by alkaline environments, chemical agents, dissolved oxygen, or enzymes to form orthoquinones, which are highly reactive toward nucleophilic alcohol, amino, or thiol groups. The resulting three-dimensional water-insoluble networks exhibit extremely high cohesive strength and multilayer morphologies. Mussel adhesive proteins do not interact with components of the human immune system, and thus may be useful in medical and surgical applications [16–18]. Unfortunately, natural mussel adhesive proteins can only be obtained in small quantities and at significant cost; for example, 10 000 mussels are needed to produce 1 g of mussel adhesive protein [7]. Synthetic polypeptides known as mussel adhesive protein analogs have been developed that mimic the properties of their natural counterparts. These materials contain L-DOPA groups similar to those in their natural counterparts [19, 20]. Mussel adhesive protein analogs have recently been modified with hydrophilic polymers in order to impart antifouling properties. For example, Dalsin and coworkers have recently described end-functionalization of poly(ethylene glycol) (PEG) with peptides that contain 1–3

DOPA groups [19]. PEG is a hydrophilic uncharged polyether that exhibits non-immunogenic and non-toxic properties. The large excluded volume, high mobility and steric hindrance properties of PEG provide PEGylated mussel adhesive protein analog materials with an ability to resist cell and protein adsorption [21–24]. For instance, PEGylated mussel adhesive protein analogs may overcome many of the environmental concerns associated with tributyltin compounds that have been traditionally used to prevent fouling of marine structures. The activity of tributyltin compounds against snails, mussels and larger mammals has led to a world-wide ban by the International Maritime Organization [25]. In addition, PEGylated mussel adhesive protein analogs may prevent non-specific adsorption of proteins on biosensors, stents, valves, catheters and other blood-contacting medical devices [26–28]. Novel procedures must be developed that allow mussel adhesive proteins and mussel adhesive protein analogs to be used in an economical manner.

In the present study, we examine thin film deposition of L-DOPA-modified poly(ethylene glycol) (mPEG-DOPA$_3$) mussel adhesive protein analog using matrix assisted pulsed laser evaporation. This process involves laser ablation of a frozen solution containing mussel adhesive protein analog and water [29–31]. The water matrix is volatile, exhibits a high vapor pressure and absorbs the laser energy. The water molecules do not deposit on the substrate because of their low sticking coefficients. On the other hand, the mussel adhesive protein analog molecules at the gas–matrix interface are ejected when kinetic energy is transferred during collisions with the water molecules. These less volatile molecules deposit on the substrate. Matrix assisted pulsed laser evaporation (MAPLE) is a physical vapor deposition process that provides control over thickness, roughness, homogeneity, and other film parameters. MAPLE is suitable for preparing organic materials, because it does not heat the depositing species. In addition, contamination is minimized when MAPLE and other processing steps are carried out within the same system. Fourier transform infrared spectroscopy, atomic force microscopy, profilometry, leachate toxicity determination and antifouling characterization were utilized to examine the structural and functional properties of MAPLE-deposited mPEG-DOPA$_3$ thin films. Our results demonstrate that MAPLE-deposited mussel adhesive protein analog films exhibit appropriate physical, chemical and antifouling properties for biomedical and marine applications.

2. EXPERIMENTAL

The DOPA-modified PEG molecule mPEG-DOPA$_3$ was synthesized using standard carbodiimide coupling chemistry in a manner described by Dalsin and co-workers [19, 20]. As seen in Fig. 1, mPEG-DOPA$_3$ is a linear PEG molecule that is end-functionalized with three DOPA end-groups. The average number of ethylene glycol repeat units in this molecule is 113. The mussel adhesive protein analog was dissolved in ethyl acetate at room temperature to prepare a 2% (g/ml) solution. The polymer solution was then pipetted into an aluminum target holder (Fig. 2).

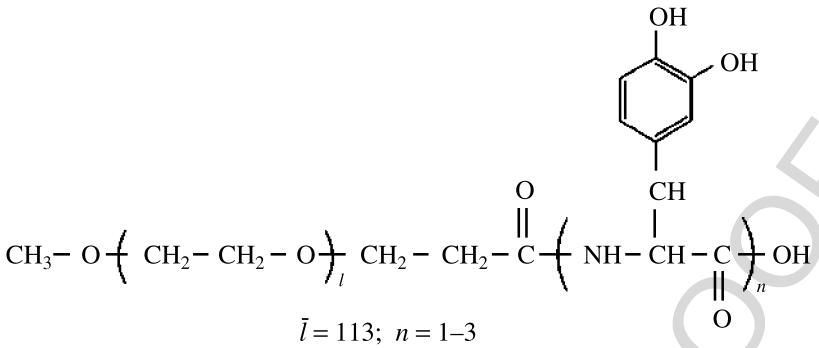

Figure 1. Chemical structure of 3,4-dihydroxyphenyl-L-alanine-modified poly(ethylene glycol) (mPEG-DOPA$_3$), which is a linear PEG molecule that is end-functionalized with three DOPA end-groups.

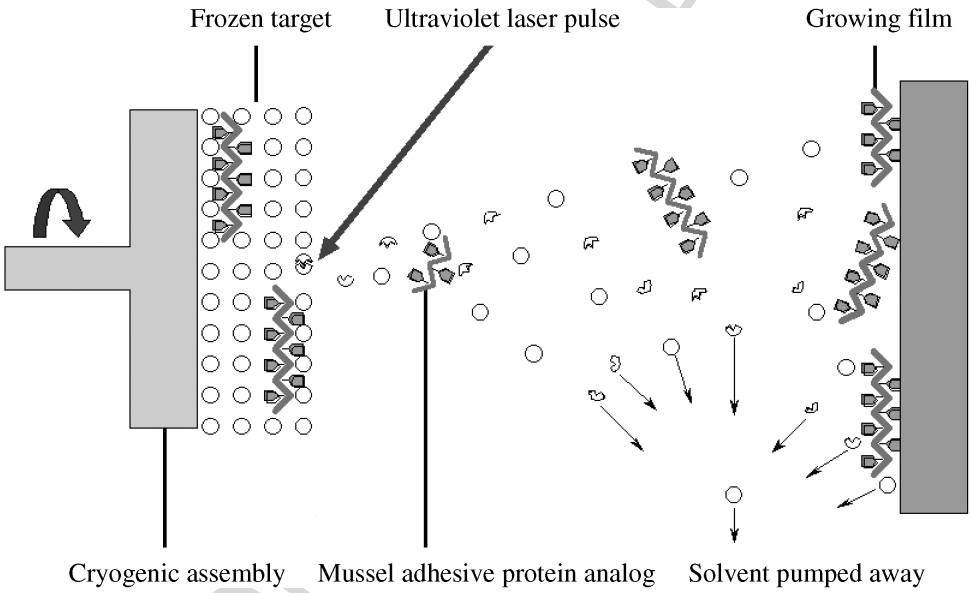

Figure 2. Schematic of the MAPLE process.

The target holder was frozen using liquid nitrogen. The frozen target was placed on a cryogenic rotating assembly within the deposition chamber. The assembly was maintained at a temperature of 173 K using copper braids that were connected to a liquid nitrogen reservoir. Several p-type silicon (100) wafers were cleaned successively in acetone and methanol ultrasonic baths. The cleaned silicon wafers and sodium chloride disks were mounted in the deposition chamber and placed at a distance of 70 mm from the target. The matrix assisted pulsed laser evaporation chamber was then evacuated to a pressure of 10^{-4} Pa. Depositions were performed using an argon fluoride excimer laser ($\lambda = 193$ nm), which was positioned at an angle of 45° with respect to the perpendicular direction from the target surface.

Table 1.
Deposition parameters for MAPLE of mPEG-DOPA$_3$ thin films

Fluence (J/cm^2)	Number of laser pulses	Thickness (nm)
0.05	50 000	0 (no film)
0.2	50 000	75
0.4	50 000	490
0.5	50 000	560
0.7	50 000	620

The target assembly was rotated at a rate of 0.4 Hz during the deposition process. The deposition parameters used in the preparation of mPEG-DOPA$_3$ thin films are provided in Table 1. Patterned films were created by placing a mask directly over the substrate during the film deposition process.

The MAPLE-deposited mPEG-DOPA$_3$ thin films were examined using Fourier transform infrared spectroscopy (FT-IR) and atomic force microscopy (AFM). Spectra were obtained from films grown on sodium chloride disks using an IFS/66 system (Bruker, Billerica, MA, USA). 100 scans were taken in the transmission mode from 4000 cm^{-1} to 600 cm^{-1} and averaged. Atomic force microscopy measurements were performed using a PicoPlus atomic force microscope (Molecular Imaging, Tempe, AZ, USA) equipped with a scanning head. Atomic force microscopy measurements were taken in the tapping mode at several resolutions. The thickness of a patterned mPEG-DOPA$_3$ thin film was examined using a Dektak stylus profilometer (Veeco/Sloan Technologies, Santa Barbara, CA, USA). The patterned MAPLE-deposited mPEG-DOPA$_3$ thin films were imaged using an IX71 inverted optical microscope (Olympus, Center Valley, PA, USA) and a digital still camera.

Leachate toxicity and biofouling studies were performed on spin-coated and MAPLE-deposited mPEG-DOPA$_3$ thin films. Uncoated aluminum and silicone elastomer 3140 (Dow Corning, Midland, MI, USA) were used as control materials in these studies. Six samples of each type were prepared in order to perform statistical analysis. Films were prepared on 15-mm-diameter sterile aluminum disks, which were secured using epoxy adhesive within the wells of a 24-well polystyrene plate, as previously reported [37]. The plate was then placed in a vented enclosure overnight to allow for curing of epoxy adhesive. 1.0 ml of sterile artificial sea water (ASW) supplemented with nutrients (0.5 g peptone and 0.1 g yeast extract per l) was added to each well. The plate was then placed on an orbital shaker at room temperature for 24 h. The leachates were collected from each well and analyzed for toxicity by incubation with *Cytophaga lytica*. An overnight culture of *C. lytica* in marine broth was harvested via centrifugation (4500 rpm for 10 min) and rinsed three times in sterile artificial sea water. Each leachate was analyzed using the dilution scheme shown in Table 2. 0.2 ml of each dilution was transferred in triplicate to a 96-well polystyrene plate and incubated at 28°C for 18 h. After rinsing and drying, 0.2 ml of the biomass indicator dye Crystal Violet (0.3%

Table 2.
Dilution scheme for leachate toxicity evaluation

Dilution (%)	Artificial seawater medium (µl)	Leachate (µl)	*C. lytica* (µl)
100	0	200	20
50	100	100	20
25	150	50	20
10	180	20	20
5	190	10	20
0	200	0	20

alcohol solution) was added to each well for 15 min and then rinsed three times with artificial sea water. 0.2 ml of 33% glacial acetic acid was added to each well and placed on an orbital shaker for 10 min to elute the Crystal Violet dye. Absorbance measurements ($\lambda = 600$ nm) were carried out to quantify the amount of *C. lytica* biofilm growth [35]. The antifouling performance of the spin-coated mPEG-DOPA$_3$ thin film, MAPLE-deposited mPEG-DOPA$_3$ thin film, uncoated aluminum and silicone elastomer surfaces was also examined. An extraction template was applied to each plate to elute the Crystal Violet dye, which was bound to the biofilm that was retained on the test surface [37]. 0.5 ml of 33% glacial acetic acid was added to each well for 10 min to release the Crystal Violet dye that was bound to the bacterial biofilm. 0.15 ml of the eluate from each well was transferred to a 96-well plate, and absorbance measurements ($\lambda = 600$ nm) were carried out.

3. RESULTS AND DISCUSSION

An attenuated total reflectance Fourier transform infrared spectrum of the MAPLE-deposited mPEG-DOPA$_3$ film (laser fluence = 0.5 J/cm^2, number of laser pulses = 50 000) is shown in Fig. 3. Several distinct bands were observed in this spectrum [32, 33]. Bands centered at 1720 cm^{-1}, 1685 cm^{-1}, 1560 cm^{-1}, 1435 cm^{-1}, 1370 cm^{-1}, 1344 cm^{-1}, 1260 cm^{-1}, 1235 cm^{-1}, 1148 cm^{-1}, 1115 cm^{-1} and 1061 cm^{-1} were observed. The peak at 1720 cm^{-1} was assigned to C=O stretching. The bands centered at 1606 cm^{-1} and 1541 cm^{-1} were attributed to aromatic ring stretching. The bands centered at 1507 cm^{-1} and 1493 cm^{-1} resulted from CH_2 shaking or wagging. The wagging process resulted from secondary interactions that allowed the material to form random coils. The peak at 1435 cm^{-1} was assigned to CH_2 deformation. The band centered at 1372 cm^{-1} was attributed to aromatic ring substitution; this band occurred in conjunction with a weak band centered at 1411 cm^{-1}. The band centered at 1235 cm^{-1} was attributed to C–O stretching in carboxylic acid groups. These results indicate that the matrix assisted pulsed laser evaporation process does not significantly alter the structure or the concentration of the main functional groups present in L-DOPA-modified poly(ethylene glycol). MAPLE deposition of mPEG-DOPA$_3$ thin films was performed at several laser

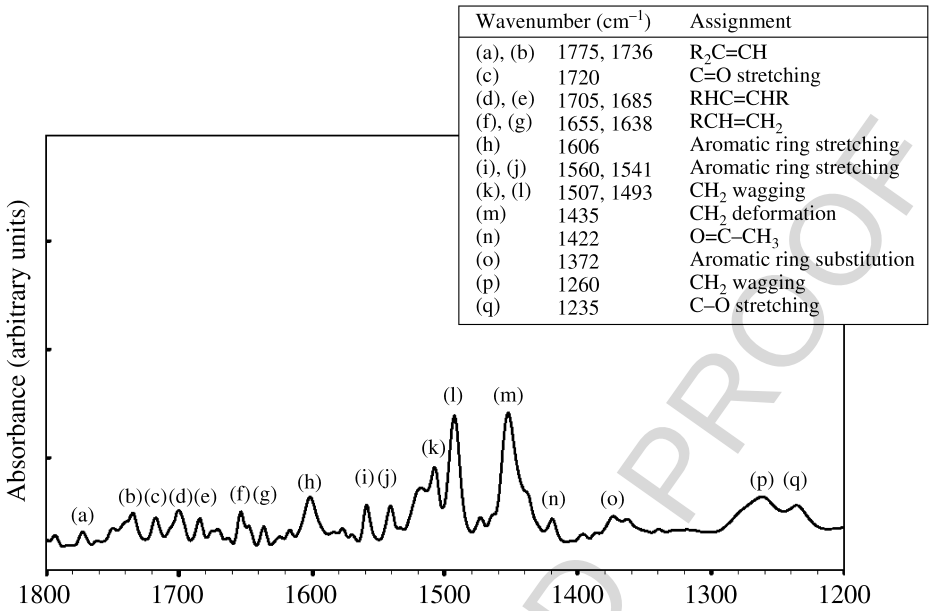

Wavenumber (cm^{-1})		Assignment
(a), (b)	1775, 1736	$R_2C=CH$
(c)	1720	C=O stretching
(d), (e)	1705, 1685	RHC=CHR
(f), (g)	1655, 1638	$RCH=CH_2$
(h)	1606	Aromatic ring stretching
(i), (j)	1560, 1541	Aromatic ring stretching
(k), (l)	1507, 1493	CH_2 wagging
(m)	1435	CH_2 deformation
(n)	1422	$O=C-CH_3$
(o)	1372	Aromatic ring substitution
(p)	1260	CH_2 wagging
(q)	1235	C–O stretching

Figure 3. High-resolution Fourier transform infrared spectrum of a MAPLE-deposited mPEG-$DOPA_3$ thin film recorded in transmission mode.

fluences in order to determine film deposition rates. MAPLE deposition at a laser fluence of 0.05 J/cm^2 did not produce a thin film that could be measured using profilometry. MAPLE deposition at higher laser fluence values (0.2 J/cm^2, 0.4 J/cm^2, 0.5 J/cm^2 and 0.7 J/cm^2) produced films with thickness values shown in Table 1. These results indicate that MAPLE deposition at higher laser fluences produced mPEG-$DOPA_3$ thin films with larger thickness values.

Masking of the substrate during MAPLE was performed in order to prepare patterned mPEG-$DOPA_3$ films. Optical micrographs of an array of circles with different diameters, a series of lines with identical thicknesses, an array of squares, and an array of radial lines with differing widths are shown in Fig. 4. The mesoscopic two-dimensional patterns maintained the dimensions and the boundaries that were provided by the masking process. Profilometry was used to examine the thickness of a MAPLE-deposited mPEG-$DOPA_3$ thin film (Fig. 5). The maximum peak-to-valley height of five consecutive sampling sites (R_z) was 529 nm; this value was attributed to the accretion of material near the edge of the mask during the MAPLE deposition process. The central region of the film exhibited a thickness of approx. 280 nm. Several laser parameters, including deposition time, fluence (laser energy over spot area), and pulse duration influence the thickness values for MAPLE-deposited films [38].

Figure 6 contains an atomic force micrograph of the MAPLE-deposited mPEG-$DOPA_3$ thin film. The film surface contained randomly oriented chains and 100–300-nm-diameter randomly distributed pores. The surface also contained

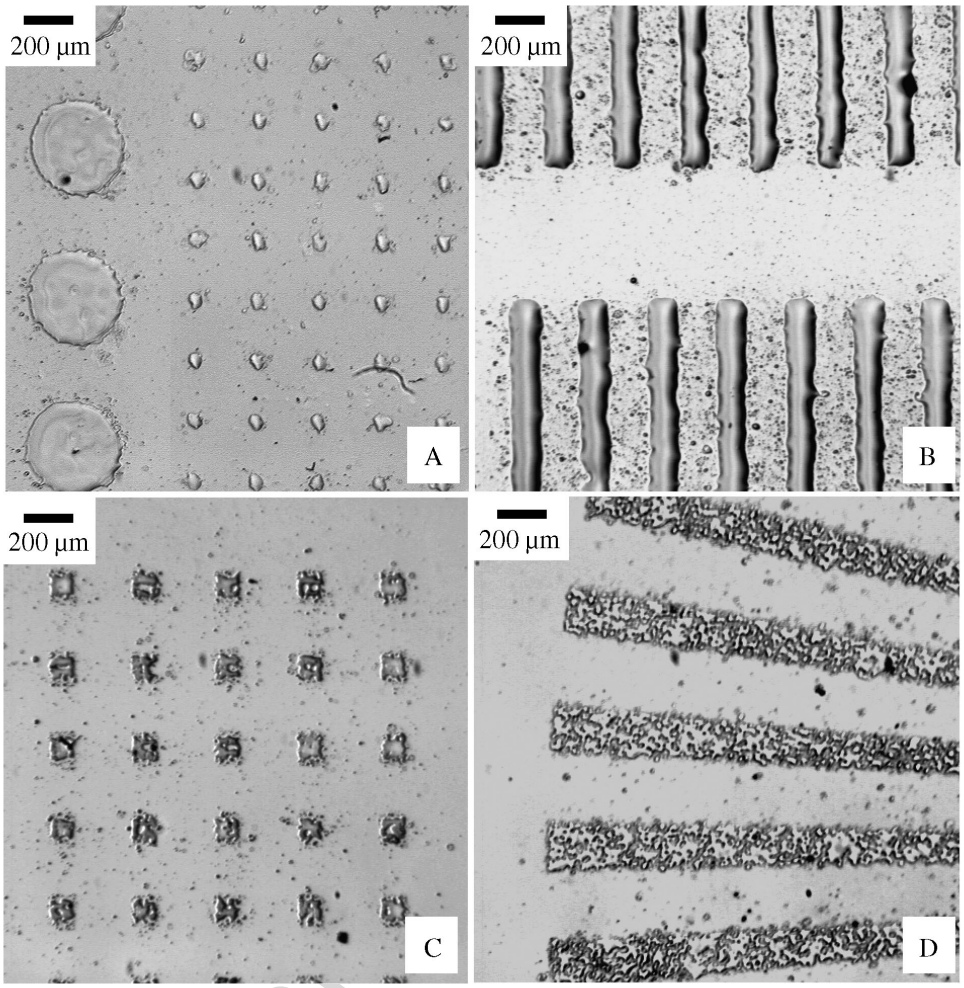

Figure 4. Optical micrographs of MAPLE-deposited mPEG-DOPA$_3$ patterns that were obtained by masking. An array of circles with different diameters, a series of lines with identical thicknesses, an array of squares, and an array of radial lines with differing widths are shown in panels A, B, C and D, respectively.

globular structures with an average size of 200 nm. These structures do not result from the matrix assisted pulsed laser evaporation process; instead, they result from "splashing" of small particles from the MAPLE target onto the substrate. This phenomenon is known to occur in pulsed laser deposition, and can be reduced by minimizing laser interaction with uneven surfaces and ablating the target with the highest possible energy density (i.e., minimizing the spot size) [35]. MAPLE has several advantages over dip coating, ink jet printing, Langmuir–Blodgett dip coating, pin arraying, spin coating and other conventional techniques for depositing biomaterial thin films. In conventional processes, droplet size and surface wetting

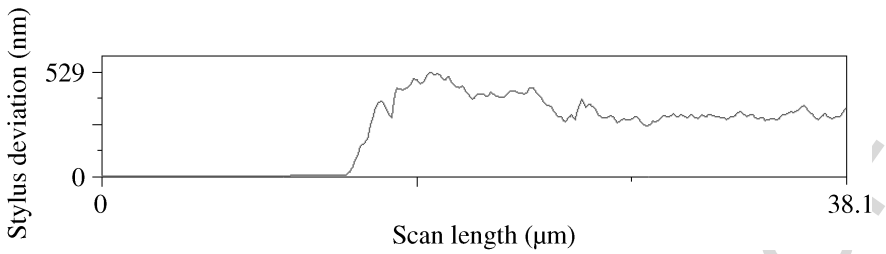

Figure 5. Profilometry results on a masked MAPLE-deposited mPEG-DOPA$_3$ pattern. Measurements were made from left (substrate) to right (film). The large R_z value (529 nm) was attributed to the accretion of material near the edge of the mask during the deposition process. The central region of the film exhibited a thickness of approx. 280 nm and relatively uniform thickness values.

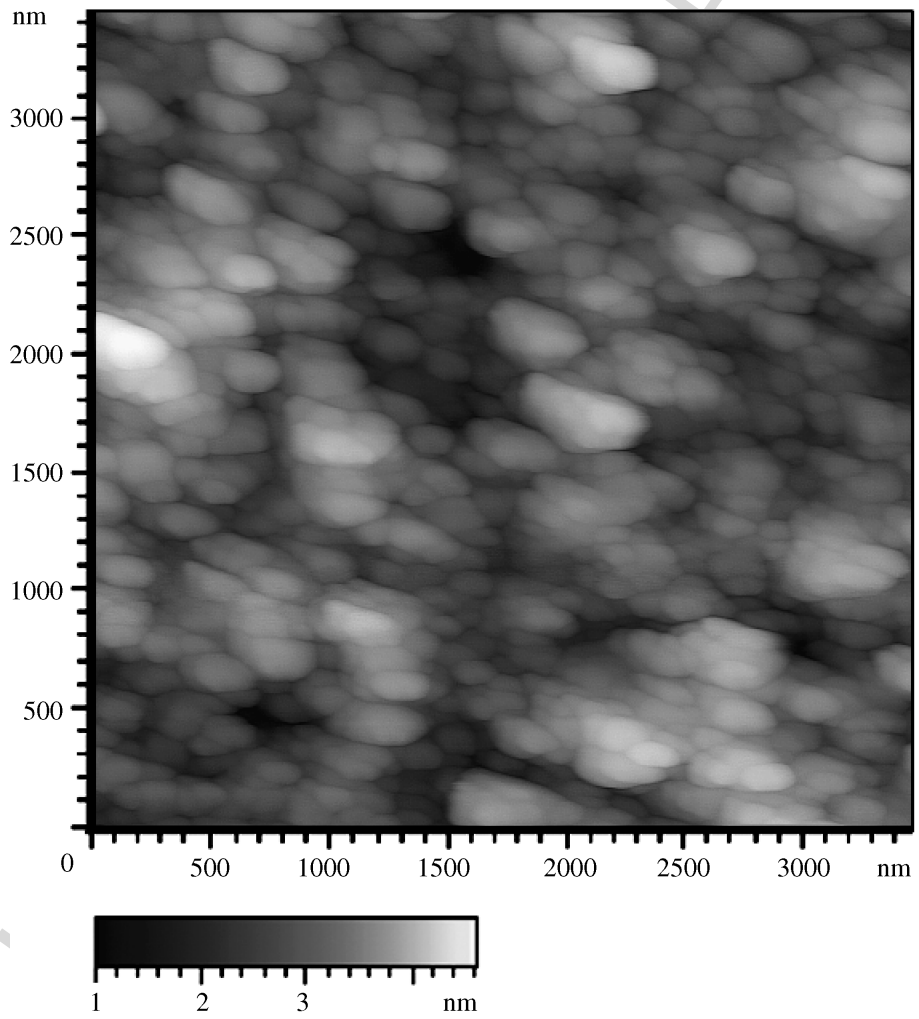

Figure 6. Topography-flattened atomic force micrograph of a MAPLE-deposited mPEG-DOPA$_3$ thin film.

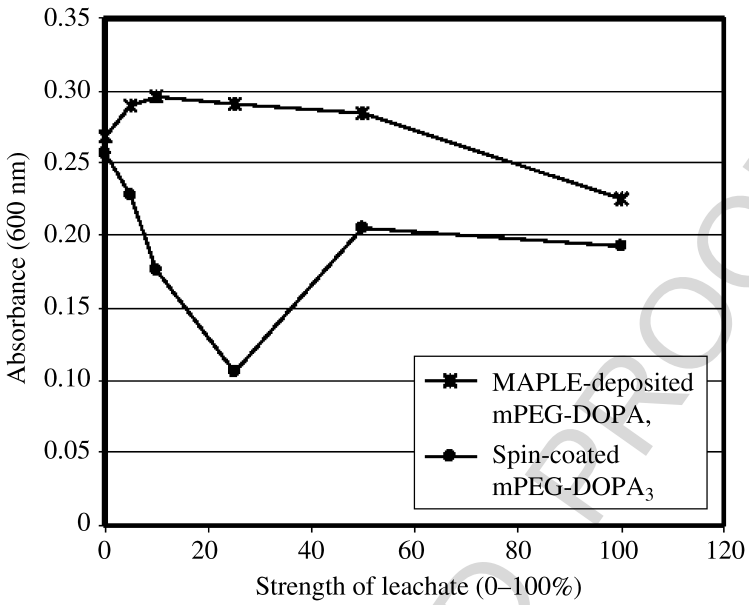

Figure 7. Coating leachate toxicity of MAPLE-deposited mPEG-DOPA$_3$ thin films obtained using *C. lytica*. Each point shown represents the mean of three replicate samples. The dilutions obtained from MAPLE-deposited mPEG-DOPA$_3$ films did not demonstrate a variation in absorbance values, which indicates that no toxic material was released from the films into the growth media. On the other hand, the dilutions obtained from spin-coated mPEG-DOPA$_3$ films exhibited a variation in absorbance values, which shows that these surfaces released toxic material into the growth media.

may affect film thickness. In addition, solvent-based processes have limitations in creating uniform films on large surfaces and in producing multilayered structures.

Leachate toxicity studies were carried out to determine if the MAPLE-deposited mPEG-DOPA$_3$ thin films immersed in artificial sea water medium released toxic materials into the surrounding environment. The results from the leachate toxicity assay are shown in Fig. 7. The amount of bacterial biofilm retained on the bottom of each well was determined using a modification of a standard photometric method [36–38]. The absorbance values were directly proportional to the amount of bacterial biofilm that was retained on the coating surface at the bottom of the well. The dilutions obtained from MAPLE-deposited mPEG-DOPA$_3$ films did not demonstrate a variation in absorbance values, which indicates that no toxic material was released from the films into the growth media. On the other hand, the dilutions obtained from spin-coated mPEG-DOPA$_3$ films exhibited a variation in absorbance values. These surfaces released toxic material into the growth media, which resulted in inhibition of *C. lytica* growth. Both MAPLE-deposited and spin-coated mPEG-DOPA$_3$ films demonstrated good antifouling performance when compared to the uncoated aluminum and silicone elastomer controls (Fig. 8). These results showed that there was less biofilm retention on the mPEG-DOPA$_3$-coated surfaces than on the uncoated control surfaces. For example, the MAPLE-

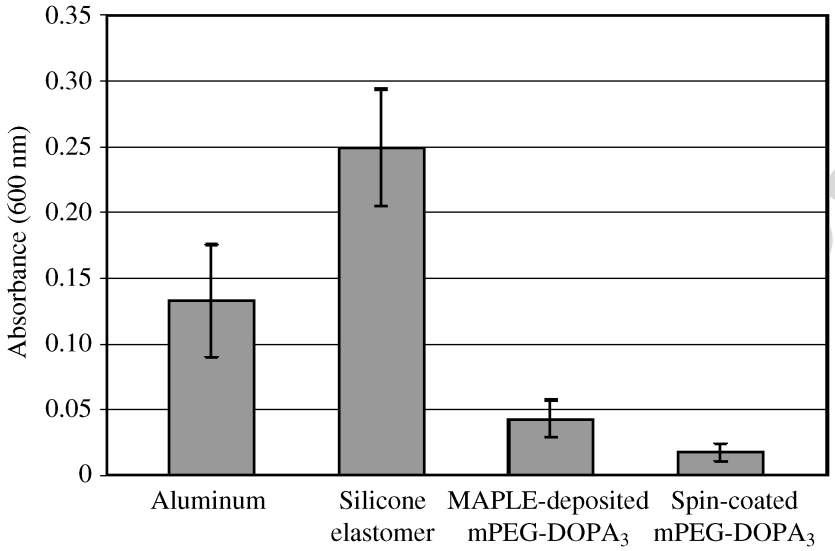

Figure 8. Antifouling performance of MAPLE-deposited mPEG-$DOPA_3$ thin films obtained using *C. lytica*. Each point represents the mean value of five replicate samples. The error bar represents one standard deviation of the mean. These results demonstrated that there was less biofilm growth on the mPEG-$DOPA_3$−coated surfaces than on the uncoated control surfaces; the spin-coated mPEG-$DOPA_3$ surfaces exhibited the lowest amount of growth.

deposited mPEG-$DOPA_3$ film demonstrated a 68% reduction in bacterial retention when compared to the uncoated aluminum control surface. Since the MAPLE-deposited mPEG-$DOPA_3$ film did not demonstrate leachate toxicity, the reduction in bacterial biofilm retention was attributed to antifouling nature of the mPEG-$DOPA_3$ material. The spin-coated mPEG-$DOPA_3$ film exhibited an 86% reduction in bacterial retention when compared to the uncoated aluminum control surface. The enhanced antifouling performance of the spin-coated mPEG-$DOPA_3$ film was attributed to the presence of leachate material in the growth medium.

4. CONCLUSIONS

Matrix assisted pulsed laser evaporation is an effective technique for preparing 3,4-dihydroxyphenyl-L-alanine-modified poly(ethylene glycol) thin films. The Fourier transform infrared spectrum from the MAPLE-deposited mussel adhesive protein analog thin film exhibits similar features to the as-prepared mussel adhesive protein analog material. Atomic force microscopy and profilometry studies suggest that MAPLE provides better control over film thickness, as well as film morphology than conventional solvent-based thin film deposition techniques. Leachate toxicity and biofouling studies suggest that MAPLE-deposited mPEG-$DOPA_3$ thin films exhibit an absence of cytotoxicity and antifouling properties against *C. lytica*. MAPLE-deposited mussel adhesive protein analog thin films may overcome several problems

associated with conventional synthetic adhesives and greatly improve wound repair in the next generation wound closure, drug delivery and fracture fixation devices. MAPLE-deposited mussel adhesive protein analog thin films could also serve as an environmentally friendly alternative to synthetic adhesives in marine applications.

Acknowledgements

The authors would like to acknowledge support from the Office of Naval Research. B. Mizaikoff, N. Menegazzo and C. Kranz are thanked for their support in atomic force microscopy imaging.

REFERENCES

1. M. Hauptmann, J. H. Lubin, P. A. Stewart, R. B. Hayes and A. Blair, *Am. J. Epidemiol.* **159**, 1117 (2004).
2. M. Hauptmann, J. H. Lubin, P. A. Stewart, R. B. Hayes and A. Blair, *J. National Cancer Inst.* **95**, 1615 (2003).
3. L. Pinkerton, M. Hein, L. Stayner and L. T. Stayner, *Occup. Environ. Med.* **61**, 193 (2004).
4. D. Coggon, E. C. Harris, J. Poole and K. T. Palmer, *J. Natl. Cancer Inst.* **95**, 1608 (2003).
5. I. C. Ennker, J. Ennker, D. Schoon, H. A. Schoon, M. Rimpler and R. Hetzer, *Ann. Thorac. Surg.* **57**, 1622 (1994).
6. D. S. Hwang, H. J. Yoo, J. H. Jun, W. K. Moon and H. J. Cha, *Appl. Environ. Microbiol.* **70**, 3352 (2004).
7. J. H. Waite, *Integr. Comp. Biol.* **42**, 1172 (2002).
8. J. H. Waite, T. J. Housley and M. L. Tanzer, *Biochemistry* **24**, 5010 (1985).
9. S. W. Taylor, J. H. Waite, M. M. Ross, J. Shabanowitz and D. F. Hunt, *J. Am. Chem. Soc.* **116**, 10803 (1994).
10. M. Yu and T. J. Deming, *Macromolecules* **31**, 4739 (1998).
11. M. Yu, J. Hwang and T. J. Deming, *J. Am. Chem. Soc.* **121**, 5825 (1999).
12. D. C. Hansen, G. W. Luther and J. H. Waite, *J. Colloid Interface Sci.* **168**, 206 (1994).
13. J. H. Waite and M. L. Tanzer, *Biochem. Biophys. Res. Commun.* **96**, 1554 (1980).
14. J. H. Waite and M. L. Tanzer, *Science* **212**, 1038 (1981).
15. D. R. Filpula, S. W. Lee, R. P. Link, S. L. Strausberg and R. L. Strausberg, *Biotechnol. Progr.* **6**, 171 (1990).
16. R. L. Strausberg and R. P. Link, *Trends Biotechnol.* **8**, 53 (1990).
17. J. B. Robin, P. Picciano, R. S. Kusleika, J. Salazar and C. Benedict, *Arch. Ophthalmol.* **106**, 973 (1988).
18. J. B. Robin, C. F. Lee and J. M. Riley, *Refract. Corneal Surg.* **5**, 302 (1989).
19. B. P. Lee, J. L. Dalsin and P. B. Messersmith, *Biomacromolecules* **3**, 1038 (2002).
20. J. L. Dalsin, L. J. Lin, S. Tosatti, J. Voros, M. Textor and P. B. Messersmith, *Langmuir* **21**, 640 (2005).
21. P. Kingshott, H. Thissen and H. J. Griesser, *Biomaterials* **23**, 2043 (2002).
22. S. I. Jeon, J. H. Lee, J. D. Andrade and P. G. de Gennes, *J. Colloid Interface Sci.* **142**, 149 (1991).
23. S. I. Jeon, J. D. Andrade and P. G. de Gennes, *J. Colloid Interface Sci.* **142**, 159 (1991).
24. I. Szleifer, *Biophys. J.* **72**, 595 (1997).
25. R. J. Huggett, M. A. Unger, P. F. Seligman and A. D. Valkis, *Environ. Sci. Technol.* **26**, 232 (1992).
26. G. M. Bruinsma, H. C. van der Mei and H. J. Busscher, *Biomaterials* **22**, 3217 (2001).

27. N. Wisniewski and M. Reichert, *Colloids Surfaces B* **18**, 197 (2000).
28. E. Ostuni, R. G. Chapman, M. N. Liang, G. Meluleni, G. Pier, D. E. Ingber and G. M. Whitesides, *Langmuir* **17**, 6336 (2001).
29. B. R. Ringeisen, J. Callahan, P. K. Wu, A. Pique, B. Spargo, R. A. McGill, M. Bucaro, H. Kim, D. M. Bubb and D. B. Chrisey, *Langmuir* **17**, 3472 (2001).
30. R. Cristescu, D. Mihaiescu, G. Socol, I. Stamatin, I. N. Mihailescu and D. B. Chrisey, *Appl. Phys. A* **79**, 1023 (2004).
31. P. K. Wu, B. R. Ringeisen, D. B. Krizman, C. G. Frondoza, M. Brooks, D. M. Bubb, R. C. Y. Auyeung, A. Pique, B. Spargo, R. A. McGill and D. B. Chrisey, *Rev. Sci. Instrum.* **74**, 2546 (2003).
32. K. Huang, B. P. Lee, D. R. Ingram and P. B. Messersmith, *Biomacromolecules* **3**, 397 (2002).
33. D. Lin-Vien, N. B. Colthup, W. B. Fateley and J. B. Grasselli, *The Handbook of Infrared and Raman Characteristic Frequencies of Organic Molecules*. Academic Press, Boston, MA (1991).
34. W. S. Tsang, C. L. Mak and K. H. Wong, *Appl. Phys. A* **77**, 693 (2003).
35. S. Stepanovic, D. Vukovic, I. Dakic, B. Savic and M. Svabic-Vlahovic, *J. Microbiol. Methods.* **40**, 175 (2000).
36. K. Merritt, A. Gaind and J. M. Anderson, *J. Biomed. Mater. Res.* **39**, 415 (1998).
37. S. J. Stafslien, J. A. Bahr, J. M. Feser, J. C. Weisz, B. J. Chisholm, T. E. Ready and P. Boudjouk, *J. Comb. Chem.* **8**, 156 (2006).
38. T. M. Patz, A. Doraiswamy, R. J. Narayan, N. Menegazzo, C. Kranz, B. Mizaikoff, Y. Zhong, R. Bellamkonda, J. D. Bumgardner, S. H. Elder, X. F. Walboomers, R. Modi and D. B. Chrisey, *Mater. Sci. Eng. C*, in press (2007).